# Electronic Supplementary Information: Confirmation of the Electrostatic Self-Assembly of Nanodiamonds

**Lan-Yun Chang,[a] Eiji Ōsawa[b] and Amanda S. Barnard*[,c]**

## Experimental

### Preliminary screening

Not all the crude agglutinates are crushable into primary particles by beads-milling. The most reliable criterion for the crushability of crude detonation product is zeta-potential in aqueous suspension, which must be higher than +50mV or lower than -50mV as determined on a Zetasizer Nano-ZS (Malvern Instruments, England). We use fluffy, grey-coloured fine powder made by Guangzhou Panyu Guangda Electromechanical Company (Guangzhou, China).

### Slurry preparation

Suspension of 10% agglutinate powder in water was prepared by agitating the mixture with a T.K.Robomix (model f, Primix Co., Tokyo) at a rotor speed of 5000 rpm for 30 min, followed by immersion into a powerful supersonic washing bath (model W-113 MK-II, Honda Electronics Co., Toyohashi) for at least two hours. At the end of this period, thick, homogeneous and light grey slurry was obtained, which soon produces dense precipitates.

### Beads-milling

The slurry prepared above is charged into a slurry reservoir of a vertical Ultra Apex Mill (type UAM-015, manufactured by Kotobuki Industries Co., Tokyo), locally modified at the reservoir portion in order to perform milling under nitrogen atmosphere and to facilitate sampling, taking out the aliquot colloid and washing. Optimum conditions of milling were determined by using Experimental Design technique under the L9 orthogonal array formalism with the following variables: diameter of zirconia beads, packing rate of beads in the milling space, slurry concentration, rotor periphery speed, and number of circulation passes.

### Intense supersonic treatment with sonotrode

The collision between freshly dispersed diamond and abundant zirconia beads in the mill should be kept at a minimum in order to suppress the etching of zirconia by diamond. For this reason, the milling cycle was cut short of complete disintegration and the final step is taken care of by irradiation of intense ultrasonic wave from a 400W laboratory ultrasonic processor (type UP-400S manufactured by Hielscher Ultrasonic Co., Germany) attached with a titanium sonotrode (type H22).

### Centrifugal separation of uncrushable residue

The sonicated colloidal solution was subjected to centrifugal separation of still remaining visible particles and other contaminants using a Table-top Centrifuge (type 5200 manufactured by KUBOTA Corporation) equipped with a swing bucket rotors (type ST-720, 200ml×4) at 3500 rpm for 1h. In average, 4.8 wt% of the used agglutinates were collected by this operation as uncrushable sediments. Supernatant liquids were collected by decantation and subjected to analysis.

### Particle-size distribution

The most useful criterion on the quality of colloidal solution is naturally the particle-size distribution. However the straightforward determination of particle size in nanocolloidal solution by means of dynamic light scattering method is unreliable and the reproducibility of results are in general unsatisfactory. We have long decided to seek a concentration range which gives the consistent size-distribution. In a typical run of a typical sample the size-distribution consists of a predominant and narrow distribution around 5nm and broad and minor peaks centred around 50-60 nm. The first peak comes from the primary particles of detonation nanodiamond but the origin of the second peak is still unknown. We used only those results where this typical pattern was obtained with reproducibility higher than 80%. In the particular sample used in this work, the particle-size distribution was determined by using three concentrations, 2.2, 2.0 and 1.8%. For each concentration, DLS measurements were repeated 440 times. The continuous series of measurements was divided into five equal sequences, and partial averages in each section are compared and the middle result with regard to the size of major peak was chosen as a representative distribution. Among the three representative results for three different concentrations, the middle one is finally chosen as the correct value. Hence the final answer is based on more than 1300 determinations, which takes about 45 min on a Particle Analyzer FPAR1000 equipped with an automatic sample FP3000 (manufactured by Ohtsuka Electronics Co., Tokyo). For the particular aqueous colloidal solution (2.0 w/v %) used in this work, distribution of the major peak was thus determined to appear at 4.1±0.5nm (99.4 wt %).

### Electron Microscopy

The analysis of the diamond nanoparticles samples was carried out using high resolution aberration-corrected transmission electron microscopy (HRTEM) operated at 80kV. In each case the images presented in the main text were supported by the Fourier transform analysis. For example, a sub-region in Figure 1 is shown in Figure S1c, where lattice image of a typical diamond nanoparticle is

---

[a] *Monash Centre for Electron Microscopy and School of Chemistry, Monash University, Clayton, VIC, Australia.*
[b] *NanoCarbon Research Institute, AREC, Faculty of Textile Science and Technology, Shinshu University, Ueda, Nagano, Japan*
[b] *CSIRO Materials Science and Engineering, Clayton, Australia. Fax: +61 3 9545 2059; Tel: +61 3 9545 7840;*
* *E-mail: amanda.barnard@csiro.au*

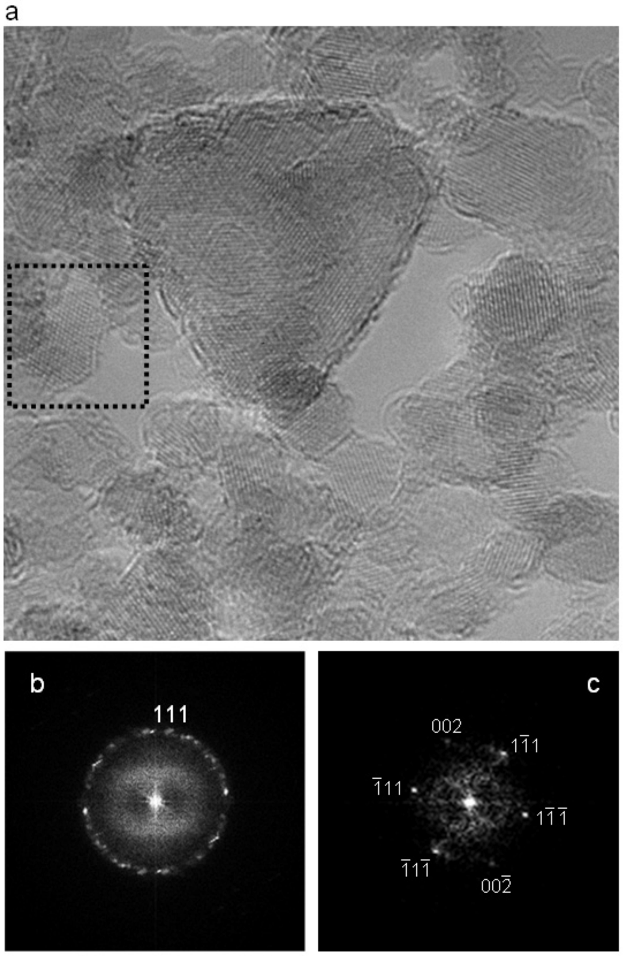

**Fig.S1. (a)** is the HRTEM image of a typical area of detonation nanodiamonds. **(b)** is the modulus of Fourier transform of figure **(a)**. The ring pattern shows that the nanodiamonds do not have preferred orientations. **(c)** is the modulus of Fourier transform of a sub-region shown in dashed square in **(a)**. The reflections were indexed and marked in **(c)**. The diamond nanoparticles in this sub-region is of [110] orientation and the weak {200} reflections, which should be forbidden in the kinematical conditions, are due to double scattering.

presented, shows strong {111} reflections and much weaker {200} reflections. Although {200} reflections are forbidden under kinematical conditions, it is well known that these "supposedly forbidden" {200} reflections are commonly observed in diamond due to double scattering [1]. In addition, the magnitude of {200} reflections in our case is much weaker than {111) reflections, which definitively confirms that the samples are members of the Fd3m space-group.

The Fourier transforms of the areas of individual nanodiamond in Figure 3 in the main text, are shown in Figure S2. These results clearly show that the diamond nanoparticles in these samples consist of a diamond structured core with fullerenic surfaces, and are absent of defects. These Fourier transforms were used to determine the orientations of the nanodiamonds (which are in [110] orientations for region 1 and 4). The strong {111} reflections (also shown in the lattice fringes in all nanodiamonds in Figure 3 of the main text), along and the angles between {111} fringes and the interface, definitively determine the interfacial planes.

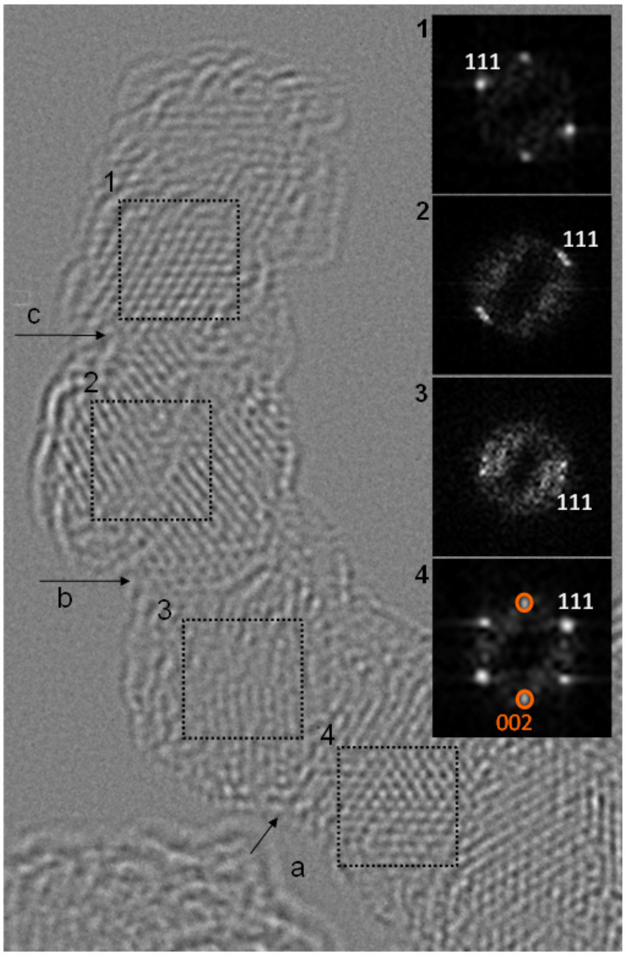

**Fig.S2.** HRTEM image of a linear chain and the corresponding moduli of Fourier transforms of individual diamond nanoparticles. The strong reflections in the Fourier transforms were measured to be {111} reflections. The Fourier transform of region 4 shows weak {002} reflections, which are due to double scattering.

In addition to this, the modulus of Fourier transform of Figure 1a (a typical area of the detonation nanodiamond) shows a case where there is no preferred orientation. This highlights that this technique is not biased toward the assumption that all nanodiamonds self-assemble, and can also identify nanodiamonds in random orientations, as shown in Figure S1b.

## Computational

To be consistent with the results (and speculations) of references 2 and 3, the present study also uses the density functional based tight binding method with self-consistent charges (SCC-DFTB) [4,5]. In this approach, a universal short-range repulsive potential accounts for double counting terms in the Coulomb and exchange-correlation contributions as well as the inter-nuclear repulsion, and self-consistency is included at the level of Mulliken charges. Although not strictly an observable quantity, the Mulliken charges are not extracted post facto, and form an integral part of the energy functional which expresses local density fluctuations around a given atom. Mulliken charge fluctuations are calculated from the eigenvalue coefficients, and are algorithmically independent from bonding considerations and spatial partitioning schemes [6]. Therefore, although they generally have limited quantitative value, they are useful in illustrating bonding trends in heteronuclear systems, and near the surface of molecules and clusters such the nanodiamonds under consideration herein [7-11].

## Acknowledgements

Computational resources for this project have been supplied by the National Computing Infrastructure (NCI) national facility under Partner Grant q27. Aberration-corrected Titan 80-300 (FEI Company) used in this project has been funded by Australian Research Council Grant LE0454166.

## References

1 J. H. Spence, *Experimental High-Resolution Electron Microscopy*, Oxford University Press, 2nd edition, 1988., pp. 144.
2 A. S. Barnard and M. Sternberg, *J. Mater. Chem*. 2007, **17**, 4811.
3 A. S. Barnard, *J. Mater. Chem*. 2008, **18**, 4038.
4 D. Porezag, Th. Frauenheim, Th. Köhler, G. Seifert and R. Kaschner, *Phys. Rev. B* 1995, **51**, 12947.
5 Th. Frauenheim, G. Seifert, M. Elstner, Th. Niehaus, C. Köhler, M. Amkreutz, M. Sternberg, Z. Hajnal, A. Di Carlo and S. Suhai, *J. Phys.: Condens. Matter*, 2002, **14**, 3015.
6 M. Scholz and H.-J. Köhler, Quantenchemische Näherungsverfahren und ihre Anwendung in der organischen Chemie, Vol. 3, Quantenchemie–Ein Lehrgang, Deutscher Verlag der Wissenschaften, Berlin, 1981.
7 G. Jungnickel, D. Porezag, Th. Frauenheim, M. I. Heggie, W. R. L. Lambrecht, B. Segall, J. C. Angus, *Phys. Stat. Sol. a* 1996, **154**, 109.
8 R. Astala, M. Kaukonen, R. M. Nieminen, G. Jungnickel, Th. Frauenheim, *Phys. Rev. B,* 2001, **63**, 814026
9 A. S. Barnard and M. Sternberg, *J. Phys. Chem. B*, 2005, **109**, 17107
10 A. S. Barnard and M. Sternberg, *Nanotech*., 2007, **18**, 025702.
11 A. S. Barnard and M. Sternberg, *J. Phys. Chem. B*, 2006, **110**, 19307.